Polymer Vol. 39 No. 24 pp. 5961–5972, 1998
0032-3861/98/$ – see front matter

PII: S0032-3861(98)00055-X

TGA–*FT*i.r. investigation of the thermal degradation of Nafion® and Nafion®/[silicon oxide]-based nanocomposites

Q. Deng[a], C.A. Wilkie[b], R.B. Moore[a] and K.A. Mauritz[a,*]
[a]*Department of Polymer Science, University of Southern Mississippi, Hattiesburg, MS 39406-0076, USA*
[b]*Department of Chemistry, Marquette University, Milwaukee, WI 53233, USA*
(Received 3 December 1996; revised 21 September 1997; accepted 19 December 1997)

The integrated TGA–*FT*i.r. technique probed the thermal degradation of: (1) a Nafion®–H^+ membrane; (2) this membrane as modified by incorporation of a $SiO_{2[1-x/4]}$ $(OH)_x$ phase via *in situ* sol–gel reactions for tetraethoxysilane; and (3) this modified membrane as further modified, organically, via post-reaction with diethoxydimethylsilane. Gravimetric loss is multistep for (1) and (2), but occurs in a single step for (3) which has the greatest thermal degradative stability. The considerable inhibition of SO_2 evolution for (2) and (3) is rationalized in terms of side-chains that are immobilized within silicon oxide cages that block reactions involving SO_3 groups. Degradation of $SiO_{2[1-x/4]}$ $(OH)_x$ 'cores' by generated HF is retarded by their organic 'shells' in (3). Substituted carbonyl fluorides and CF_2-containing fragments appear. Si-CH_3 and CH_3 groups and/or –CH=CH_2 vinyl compounds are degradation products for (3). It is unlikely that intact R-SO_2-OH groups, or perfluoroalkylether groups issuing from the side-chains of Nafion®, exist as gas phase products. The origins of some peaks are in question owing to spectral complexity. Altogether, the hybrid (3) is superior with respect to degradation onset temperature, subsequent mass loss over a range of about 100°C, and low quantity of evolved products.

(Keywords: TGA–*FT*i.r.; thermal degradation; Nafion®/[silicon oxide])

INTRODUCTION

The nanophase-separated morphology of Nafion® membranes has been exploited as a morphological template for *in situ* sol–gel reactions of tetraethoxysilane (TEOS = $Si(OC_2H_5)_4$) and TEOS-DEDMS (DEDMS = diethoxydimethylsilane = $(CH_3)_2Si(OC_2H_5)_2$) mixtures to create Nafion®–[silicon oxide] and Nafion®–[organically modified silicate] hybrid materials[1]. Nafion® is a perfluorosulfonate ionomer whose morphology consists of 3–5 nm clusters of $-SO_3^-X^+$ (X = H or cation)-ended perfluoroalkylether side-chains that are dispersed throughout a semicrystalline tetrafluoroethylene matrix[2]. Hydrolysed alkoxy- and/or alkylalkoxysilane molecules migrate to the clusters which serve as reactors in which hydrolysis is catalysed by -SO_3H groups, and in which the sol–gel reaction initiates and inorganic oxide or organically modified silicate nanoparticles are formed upon drying. In another scheme[3], $SiO_{2[1-x/4]}$ $(OH)_x$ nanoparticles were generated via *in situ* sol–gel reactions for TEOS within clusters. Then, residual SiOH groups on these nanoparticles, or 'cores', were post-reacted with DEDMS resulting in organically-'shelled' and covalently interknitted nanoparticles, as depicted in *Figure 1*. SAXS studies[4,5] established that the morphology of unfilled Nafion® persists after its invasion by the sol–gel-derived phase. Molecular structure was characterized within these silicon-containing nanophases using *FT*i.r. and ^{29}Si solid state NMR spectroscopies[1,6]. Pyrene photophysical probes interrogated structural polarity within Nafion®–SiO_2 and Nafion®–[organically modified silicate] hybrids[7]. DSC analysis revealed that T_m for Nafion®–SiO_2 is greater than that for pure Nafion®–H^+[8]. Dynamic mechanical spectra for Nafion®–SiO_2 show an increase in a weak glass-like transition temperature, as well as in T_m, relative to Nafion®–H^+[8]. Nafion®–SiO_2 has greater tensile strength and lower ductility than Nafion®–H^+[8]. A general conclusion issuing from these thermal–mechanical studies is that the molecular chains in Nafion® are rendered less mobile by their interactions with the sol–gel-derived filler. In turn, hindered chain segmental motion has implications with regard to the thermal degradative stability, which is the theme of the work presented here.

Hyphenated techniques for characterizing thermal degradation of polymers, such as TGA-*FT*i.r. and TGA-mass spectrometry, are becoming increasingly important[9]. The temporal resolution of specific fragments in the gas phase concurrent with mass loss measurement is of importance in analysing degradation mechanisms. It is particularly important that quantitative analysis may be performed using this technique when more than one component is pyrolysed during a single observed weight loss step[10].

Here, we report TGA–*FT*i.r. results for the thermal degradation of: (1) a Nafion®-H^+ membrane; (2) this membrane as modified by the incorporation of a silicon oxide phase via *in situ* sol–gel reactions for TEOS; and (3) the $SiO_{2[1-x/4]}$ $(OH)_x$-filled membrane as post-reacted with DEDMS. Degradation products issuing from the base

* To whom correspondence should be addressed. Tel:001 601 266 5595; Fax: 001 601 266 5504.

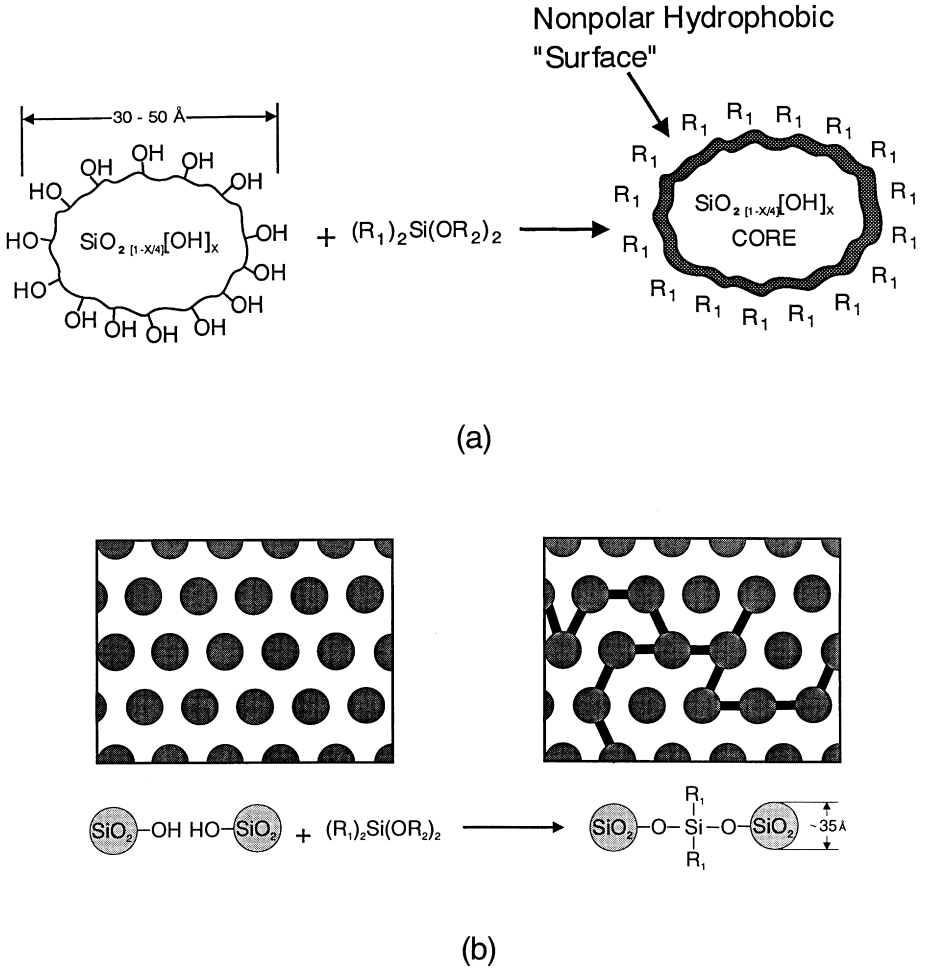

Figure 1 (a) Silicon oxide nanoparticles that are imparted hydrocarbon 'shells' by post-reaction of SiOH groups with DEDMS. (b) Depiction of an array of isolated $SiO_{2\,[1-x/4]}\,(OH)_x$ nanoparticles (left), and the same particles, but interknitted by $[\text{-O-Si}(R_1)_2]_n\text{-O-}$ bridges by condensation reactions (right). $n = 1$ in the figure

polymer must derive from the following chemical structure:

$$[CF_2CF(CF_2CF_2)_n]_m,$$
$$\backslash$$
$$OCF_2CFCF_3$$
$$\backslash$$
$$OCF_2CF_2SO_3H$$

Earlier, the thermal degradation of Nafion®-H^+ was monitored via coupled TGA–*FT*i.r. by Wilkie *et al.*[11]. A degradation mechanism was proposed involving initial cleavage of the C–S bond leading to SO_2, an ·OH radical and a carbon-based radical which undergoes further degradation.

The dependence of the thermal degradative stability of Nafion® on the nature of the SO_3 group counterion was studied by Feldheim *et al.*[12] who found that stability improves as counterion size decreases. This was attributed to an initial decomposition reaction strongly influenced by the strength of $SO_3^- X^+$ electrostatic interactions. A multi-step decomposition was observed.

Stefanithis and Mauritz[13] found that significant chemical degradation of sol–gel-derived Nafion®–SiO_2 nanocomposites begins at ~350°C and proceeds in at least three stages for both filled and unfilled Nafion®–H^+. The TGA thermogram for the unfilled form is essentially the same as that reported by Wilkie *et al.*[11]. The gradual loss of ~5 wt.% from 30 to 350°C was attributed, mainly, to volatilization of bound MeOH and H_2O. The percent of initial weight remaining at 650°C is generally less than SiO_2 uptake percent. This phenomenon will be addressed in the studies described here.

More recently, Samms *et al*. reported a coupled TGA-mass spectrometry investigation of Nafion®[14]. As seen in other studies, serious mass degradation initiates around 350°C.

Given that Nafion® is already a thermally-robust material, the enhancement of this important property is significant within the context of its present and projected uses in membrane separations in harsh environments.

EXPERIMENTAL

Materials

Equivalent weight of 1100, 5 mil thick, membranes in the K^+ form (Nafion® 115) were supplied by E.I. DuPont Co. TEOS, DEDMS and methanol were all obtained from Aldrich Chemical Co. All water utilized was distilled–deionized.

Sample Preparation

An unfilled dry Nafion®–H^+ membrane was used as an experimental control sample. Details of the formulation of

Nafion®–SiO_2 and Nafion®–[SiO_2/DEDMS-*post-reacted*] nanocomposite membranes were presented earlier[1,3] so only a brief summary is given below.

Unfilled Nafion®-H^+. First, Nafion®–K^+ membranes were converted to the sulfonic acid form by refluxing in 50% (v/v) HCl for 12 h. Then, the membranes were refluxed for 6 h in distilled–deionized water to leach out excess acid, followed by a sequence of wash steps as described earlier[3]. These samples were then dried at 100°C under vacuum for 24 h. All membranes were reduced to this *standard initial state* prior to conducting the *in situ* sol–gel reaction for the purpose of achieving maximum sample reproducibility.

Nafion®–SiO_2 Hybrids. Some of the membranes, initialized as described earlier, were immersed in stirred solutions of 3:1 (v/v) MeOH:H_2O at 22°C for 20 h. The sorbed water, serving to initiate TEOS hydrolysis, was introduced such that H_2O:TE0S = 4:1 (mol/mol) overall. Methanol is a good swelling agent for Nafion® that promotes TEOS permeability. Solutions of TEOS:MeOH = 3:1 (v/v) were added to the stoppered containers while stirring was maintained. After specified times, the membranes were removed, washed in MeOH for 1–2 s, blotted and dried at 100°C under vacuum for 24 h to remove trapped volatiles and promote further condensation of SiOH groups within the *in situ* silicon oxide phase. At this point, for these particular dried weight uptakes, isolated silicon oxide 'cores' exist within the ionomer template, as discussed earlier[3,5]. The Nafion®–SiO_2 sample used for TGA–*FT*i.r. study had 13.4 wt.% silicon oxide uptake.

Nafion®–[SiO_2/DEDMS-post-reacted] hybrids. The same dried-annealed Nafion®–SiO_2 (13.4%) hybrid described earlier was divided into several pieces. First, one piece was pre-swollen in MeOH at 22°C for 24 h to enhance permeation of DEDMS and the delivery of DEDMS molecules to reactive sites on the surfaces of in-place silicon oxide nanoparticles. DEDMS was then added to this stirred MeOH bath. After 30 min, the membrane was removed and washed for 1–2 s in pure MeOH, then surface-blotted. Afterward, the sample was placed on a Teflon®-coated plate which was transferred to a vacuum oven held at 40°C and subsequently heated to 100°C within 40 min (no vacuum). This heating was intended to promote condensation between unreacted SiOH groups and sorbed DEDMS molecules. Finally, the samples were dried-annealed at 100°C under vacuum for 24 h to remove volatiles and promote further postcondensation reactions. The percent weight uptake after post-reaction was 4.5%. All samples were kept in a desiccator prior to the TGA–*FT*i.r. experiments. No membrane surface-attached silica layers, which would complicate the IR spectra, were observed by light microscopic inspection.

TGA–FTi.r. instrumentation. Alone, TGA provides useful quantitative information regarding the thermal decomposition of polymers by monitoring mass loss events that are induced by increasing temperature. However, to identify polymer molecular fragments that evolved during a TGA experiment, it is necessary to couple this instrument to another analytical device, in this case an infrared spectrometer. The combination of TGA and *FT*i.r. is quite favourable because all evolved gases from the TGA instrument are sent to an *FT*i.r. spectrometer using a heated transfer line. Acquired spectra are compared with reference spectra stored in data banks for chemical group identification. Moreover, this hyphenated technique not only shortens analysis time but also permits analysis to be performed on the same specimen, thus minimizing experimental errors due to sample composition variation.

A Cahn thermogravimetric analyser was coupled to a Mattson Instruments Galaxy Fourier Transform Infrared Spectrometer. The evolved gases were sampled by a sniffer tube which extends into the TGA sample cup and admits only some of the gases into the analyser. The use of a sniffer tube leads to less dilution of the degradation products by the TGA purge gas. The weight of the samples ranged from 14 to 32 mg. Samples were heated from 25 to 650°C where the heating rate was 20°C min^{-1} with a 30–50 cm^3 min^{-1} inert gas purge using N_2. Evolved gases were transferred to a heated 10 cm gas i.r. cell by a heated quartz transfer line. FTIR spectra were collected at 4 cm^{-1} resolution and were baseline-corrected. Owing to the fact that we have described this technique and equipment in numerous previous papers, the reader is referred to this literature for further details[15–21]

RESULTS AND DISCUSSION

TGA thermograms for unfilled dry Nafion®–H^+, Nafion®–SiO_2 and Nafion®–[SiO_2/DEDMS-*post-reacted*] samples are displayed in *Figure 2*. Owing to the fact that the decomposition profiles are different from each other, it is concluded that the thermal degradation process of Nafion® is modified by incorporation of these sol–gel derived phases in the polar clusters. The profiles for unfilled Nafion®–H^+ and Nafion®–SiO_2 indicate that decomposition occurs by more than one step for these variants. However, from this gravimetric perspective, degradation appears to proceed in a single step for the Nafion®–[SiO_2/DEDMS-*post-reacted*] hybrid. The initial stage of degradation for Nafion®–H^+ (300°C–450°C) begins at a temperature lower than the temperatures for the onset of degradation of the two hybrids. On the other hand, the final mass loss stage for Nafion®–H^+ is extended to higher temperatures as compared with that of each of the hybrids. The two filled samples decomposed faster than Nafion®–H^+ after 450°C. Finally, the weight surviving at 650°C is ordered amongst the samples as follows: unfilled Nafion®–H^+ < Nafion®–SiO_2 < Nafion®–[SiO_2/DEDMS-*post-reacted*].

The weight loss that occurs between 300 and 400°C is the most critical not only because this is the temperature range wherein failure is initiated, but because the membrane loses its ion exchange functionality from which its important membrane properties arise. Clearly, in *Figure 2*, the Nafion®–SiO_2-PR-DEDMS curve is appreciably above the other two curves over a temperature range of about 100°C after which, somewhat above 400°C, crossover with the unfilled Nafion® curve occurs.

In theory, it would be useful in our interpretations if TGA derivative peaks, signifying inflection points, could be correlated to the various peaks corresponding to specific molecular fragments on the i.r. absorbance *versus* temperature curves which will be discussed below. Unfortunately, derivative peaks, as such, do not exist for either of the three samples, save for a minor feature on the Nafion®–H^+ curve with maximum at ~375°C. Perhaps this is a significant result in itself in the following sense: There are a number of series–parallel degradation reactions that sum up to generate the TGA curves but they are unresolvable for these systems. On the other hand, while the individual chemical processes are obscured in the gravimetric analysis,

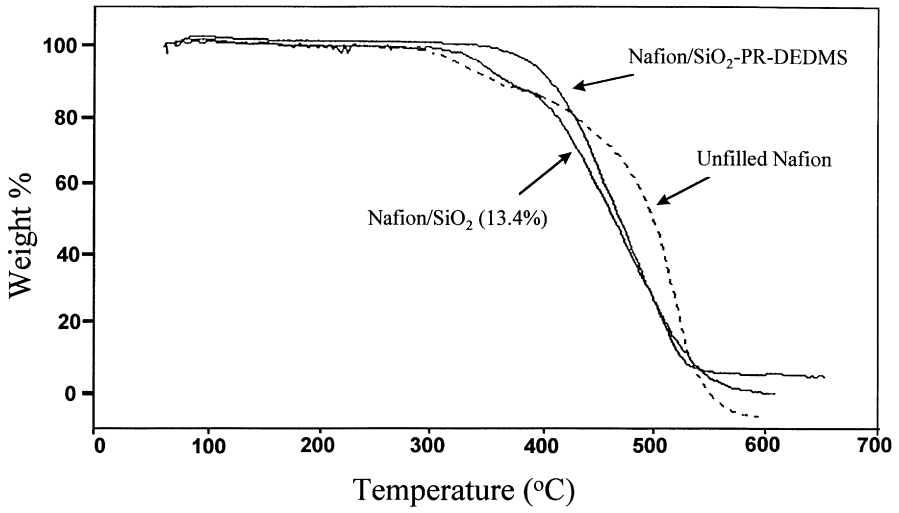

Figure 2 TGA thermograms for dry, unfilled Nafion®–H^+ and Nafion®–SiO_2 and Nafion®–[SiO_2/DEDMS-post-reacted] hybrids

the *FT*i.r. probe possesses molecular sensitivity although the unambiguous assignment of peaks is difficult for these complex systems, as will be seen.

Gases evolving from the materials were monitored by *FT*i.r. while the sample was heated within the TGA oven. The transfer of gases from TGA to *FT*i.r. instruments is rapid and with no tailing. An important strength of the integrated TGA–*FT*i.r. analysis is the ability to display gas component evolution profiles in real time on exactly the same time line as the TGA weight loss profile.

A series of spectra were collected over the time–temperature range for each TGA experiment that generated the curves in *Figure 2*. The following examples of spectra that were obtained for gaseous products are displayed in *Figure 3*: Nafion®–H^+ at 516°C (a); Nafion®–SiO_2 at 506°C (b); Nafion®–[SiO_2/DEDMS-*post-reacted*] at 514°C (c). On inspection of *Figure 3a–c*, it is clear that, at approximately the same temperature, the evolved gas compositions are not the same for the three materials.

Due to the considerable number of gas phase products that generate numerous i.r. bands, we divide the discussion of results into three parts: (1) main evolved gases (SO_2 and SiF_4); (2) other selected gas phase products; and (3) i.r. bands unique to the Nafion®–[SiO_2/DEDMS-*post-reacted*] hybrid.

SO_2 and SiF_4 gas evolution

SO_2 and SiF_4 gases have strong absorbances at ~1324 and ~1025 cm^{-1}, respectively[11], and were monitored according to these band assignments as a function of temperature. SO_2 issues from degradation of the -SO_3 groups in the polar clusters of Nafion®. These clusters act as physical cross-links that account in large measure for the very good mechanical, thermal and solvent stability of these polymers. Thus, the structural integrity of these materials is directly linked to SO_3 group stability. SiF_4 derives from a reaction between HF, that is evolved from decomposition of the side-chains and/or backbones, and silicon oxide-nanoparticles in the clusters as well as with SiO_2 in the TGA quartz tube, according to the reaction $4HF + SiO_2 \Rightarrow SiF_4 + 2H_2O$. Product CO_2 (2345–2350 cm^{-1}) is not discussed here due to uncertainties and complexities raised by the possible presence of atmospheric CO_2 in the chamber.

Gas phase absorbances for the three materials are plotted as a function of temperature in *Figure 4* for the signature bands of SO_2 (a) and SiF_4 (b). Absorbances are reduced to a per gram of Nafion® basis, i.e. the sol–gel-derived filler has been computationally deleted based upon its measured weight fraction in the given composite. Decomposition is essentially initiated by products generated within the Nafion® template instead of within either silicon oxide or organically-modified silicon oxide phases. Such a computational adjustment is logical for composites in which the filler does not degrade. However, for the hybrids considered here, the filler (as well as TGA quartz tube) can undergo the aforementioned reaction with product HF. On the other hand, the amount of SiF_4 evolved is directly related to, or is diagnostic of the amount of HF issuing from degraded Nafion®. In addition to the SiF_4 reaction, condensation reactions between residual SiOH groups by heating will reduce the mass of the filler by generating H_2O.

Nafion®–H^+. As seen in *Figure 2*, unfilled Nafion®–H^+, after a gradual, low net weight loss, initiates a first stage of chemical decomposition at ~300°C. While the spectral monitor in our experiments was applied to catastrophic chemical degradation at higher temperatures, Samms *et al.*[14] and Wilkie *et al.*[11] demonstrated that loss from 75°C to 250°C involved residual water. Then, around 6% loss occurred in the interval 300°C–340°C, 18% loss accumulated up to 420°C, 35% up to 480°C and 100% up to 560°C. Nafion® commences degradation after melting occurs in crystalline tetrafluoroethylene regions.

Numerous spectra were recorded over the temperature range *ca.* 250°C–650°C. Up to ~400°C, little SO_2 and SiF_4 was observed and from 400°C to ~480°C these products evolved slowly. For both gases, an increase in rate occurred after ~480°C with absorbances rising sharply to respective maxima around 615°C. Samms *et al.*[14] observed that the mass spectrum signal for HF was detected only above 450°C; this fact is in harmony with the onset of rapid SiF_4

Figure 3 I.r. spectra of gas phase degradation products for: (a) Nafion®–H^+ at 516°C; (b) Nafion®–SiO_2 at 506°C; and (c) Nafion®–[SiO_2/DEDMS-*post-reacted*] at 514°C. Prominent peak wavenumbers are indicated

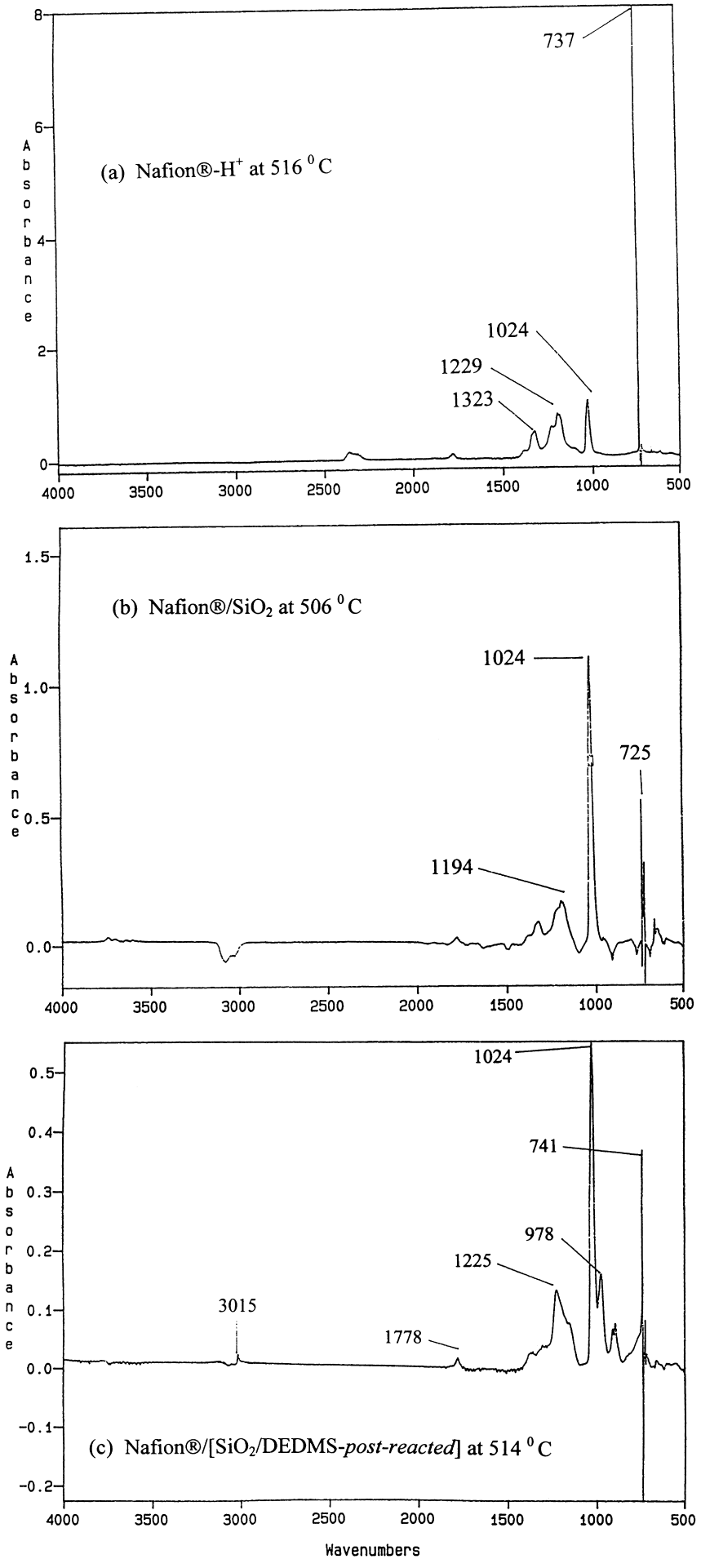
(a) Nafion®-H+ at 516 °C
737
1024
1229
1323
(b) Nafion®/SiO2 at 506 °C
1024
725
1194
(c) Nafion®/[SiO2/DEDMS-post-reacted] at 514 °C
1024
741
978
1225
3015
1778
Absorbance
Wavenumbers
4000
3500
3000
2500
2000
1500
1000
500

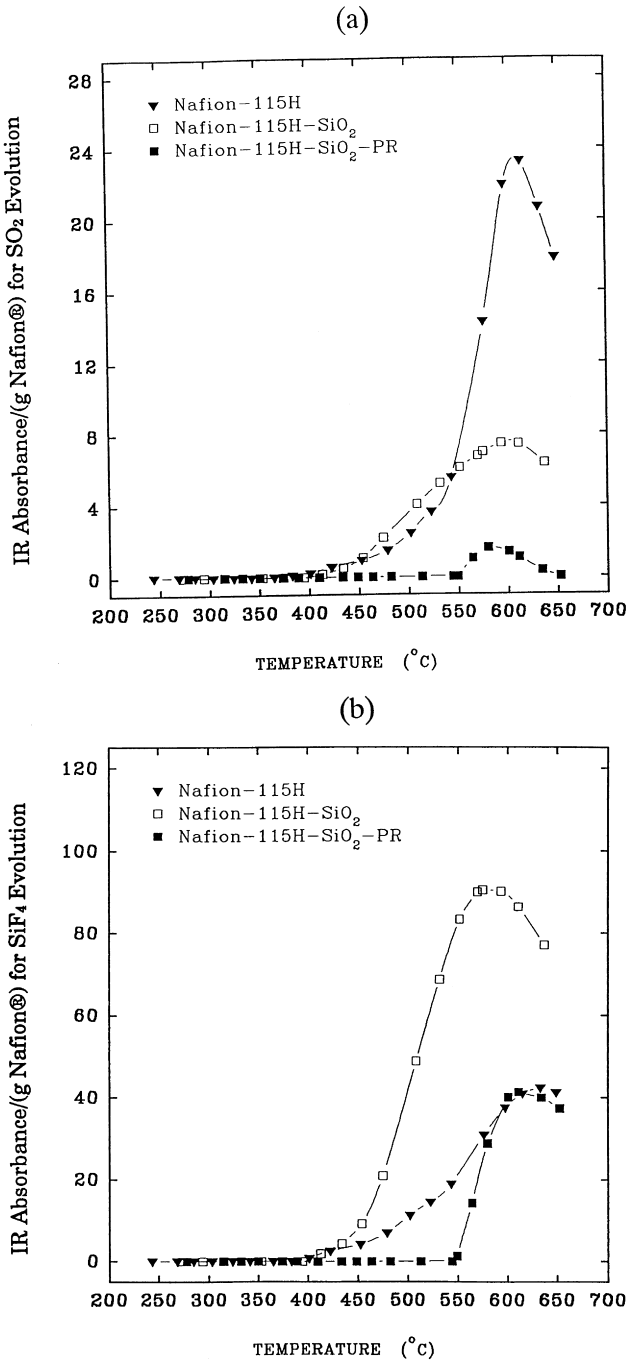

Figure 4 I.r. absorbance of: (a) SO_2 and (b) SiF_4 gas phase products *versus* temperature for Nafion®–H^+, Nafion®–SiO_2, and Nafion®–[SiO_2/DEDMS-*post-reacted*]

evolution around this temperature through the agency of HF attack. Over the investigated temperature range, neither CO(2100 cm^{-1}) nor *substituted* carbonyl fluoride (1957, 1928 cm^{-1}) absorbances were seen.

These results differ somewhat from those of Wilkie *et al.*[11] who noted a 7% loss from 280°C to 355°C such that SO_2 and CO_2 production increased while water release decreased. They noted that SiF_4, CO, HF, substituted carbonyl fluorides and C–F stretching bands all appeared in this region. In contrast, SO_2 as well as CO evolution decreased dramatically at 365°C to become insignificant. Major decomposition products in the range 355°C–560°C were HF, SiF_4, carbonyl fluorides, and species exhibiting C–F stretching vibrations.

A proposed mechanism involves initial cleavage of the C–S bond leading to SO_2, ·OH radicals, and a carbon-based radical which further degrades. The materials employed by Wilkie *et al.* in these earlier studies were Nafion®–H^+ beads and films provided by E.I. DuPont Co. without further modification. Observed differences in the results of the two studies might arise from Nafion® sample pre-history as well as equivalent weight and degree of crystallinity variance. The significant difference between the two results is that the studies reported here show a large increase in SO_2 that culminates in a maximum at 615°C whereas the sample in the earlier studies exhibited a dramatic decrease in SO_2 evolution at ~365°C Here, few C–S bonds appear to be broken before 365°C for Nafion®–H^+.

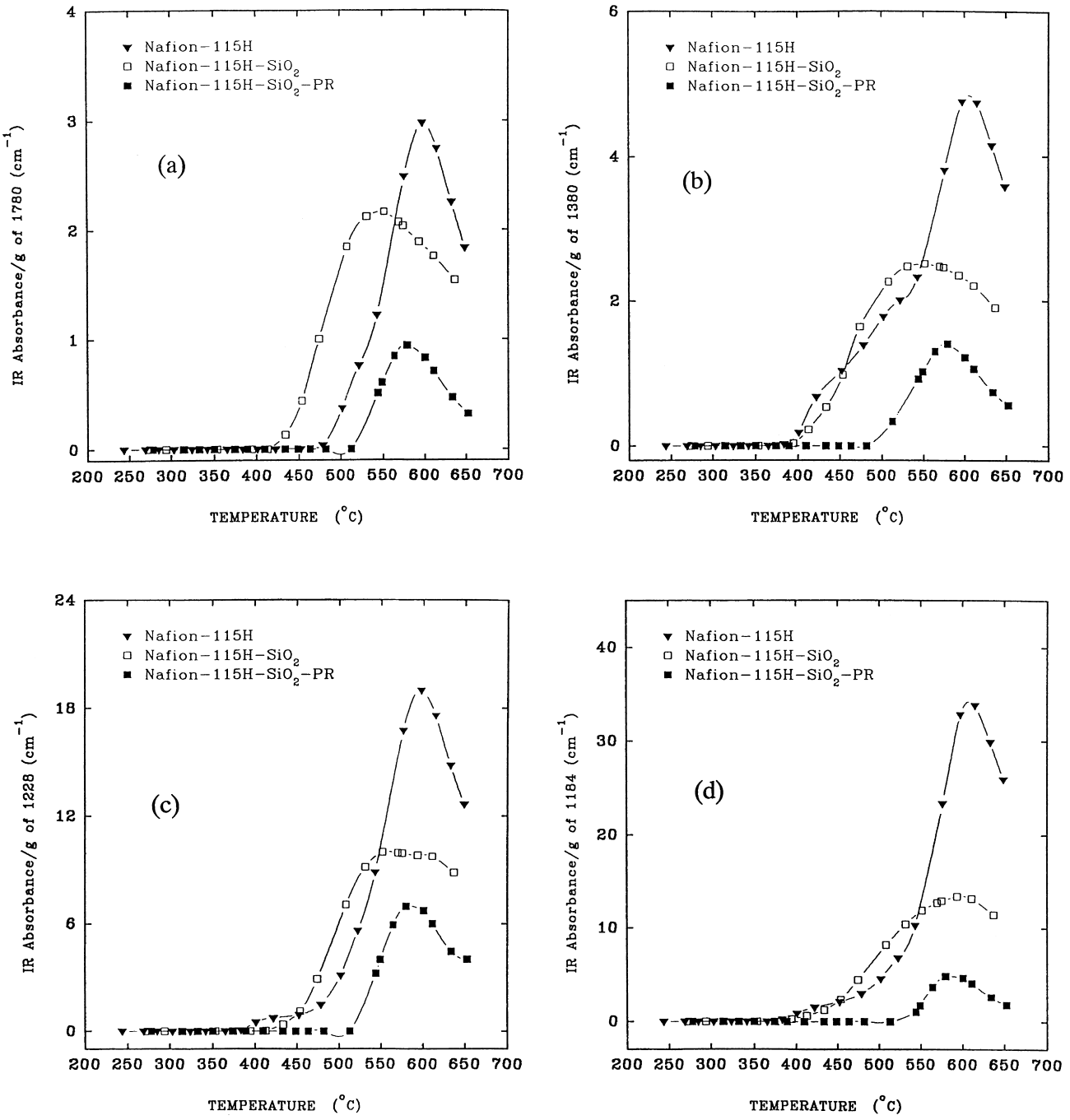

Figure 5 Same as *Figure 4*, but for bands at 1780, 1380, 1228 and 1184 cm^{-1}

Nafion®–SiO_2. Unfilled Nafion®–H^+ decomposes slower, overall, than Nafion®–SiO_2. Both Nafion®–H^+ and Nafion®–SiO_2 have at least two distinct chemical degradation steps (following initial gradual volatile release), while Nafion®–[SiO_2/DEDMS-*post-reacted*] is unique in having but one abrupt step. On the other hand, the latter clearly has the highest thermal stability (60°C–70°C upward shift), under both N_2 and air.

Compared with Nafion®–H^+, Nafion®–SiO_2 initiated decomposition 5°C–10°C higher (~305°C-310°C), but then degraded faster (*Figure 2*). At 454°C, there is a cumulative weight loss of 40%; 6.6% of the original sample weight remained at 539°C and 1.2% at 605°C.

Figure 4 shows that, up to ~454°C, only small quantities of SO_2 and SiF_4 are generated. Thereafter, SO_2 evolution uniformly increases to a maximum which is, however, considerably lower than that for unfilled Nafion®. A great increase in SiF_4 evolution takes place from 454°C to a maximum ~575°C. In the light of prior comments regarding SiF_4 evolution during the experiment with unfilled Nafion®–H^+, the results for Nafion®-incorporated SiO_2 are confusing.

Nonetheless, the fact that this sample generates more SiF_4 than unfilled Nafion® is not surprising since it is filled with a silicon oxide component that is immediately accessible for reaction with generated HF. Compared with unfilled Nafion®–H^+, SO_2 evolution is significantly reduced at higher temperatures, although at lower temperatures Nafion®–SiO_2 actually generates discernibly more SO_2. Over the studied temperature range, CO (2100 cm^{-1}) and substituted carbonyl fluorides (1957, 1928 cm^{-1}) were not observed.

The considerable inhibition of SO_2 evolution is rationalized within the context of intimate silicon oxide incorporation within nanometers-in-size clusters of $-SO_3^-$-terminated side-chains.

Silicon oxide invasion of Nafion® to this degree (13.4 wt.%) is thought to disrupt neither cluster structure nor TFE crystallinity significantly; the Bragg spacing corresponding to the SAXS 'ionomer' peak for Nafion® is essentially unchanged upon silicon oxide incorporation via the *in situ* sol–gel process[5]. Side-chains are envisioned as being immobilized within silicon oxide cages that retard reactions involving -SO_3 groups. This concept was also proposed to explain the highly polar environment sensed by pyrene fluorescence probes embedded within cluster-incorporated silicon oxide phases of Nafion®[7]. These cages, however, can be degraded by internally-generated HF which ultimately leaves side-chains unprotected. While backbone crystallinity might not be directly affected by the filler, the rate of degradation after final melting might be influenced by filler-modified interactions between side-chains within clusters. While $-SO_3^-$ groups are temporarily protected by the inorganic cages during heating, perhaps insertion of silicon oxide molecular fragments between individual side-chains might disrupt the physical cross-linking provided by side-chain aggregation. Therefore, immediately following degradation of the inorganic cages by liberated HF, the thermal decomposition of Nafion® occurs more abruptly, as seen in *Figure 2*.

It is natural that, for Nafion®–SiO_2, evolved HF would react with the membrane-internal SiO_2 component first, after which it would attack the TGA quartz sample tube. In fact, in *Figure 4* it is seen that there is more SiF_4 generated for Nafion®–SiO_2 than for unfilled Nafion®–H^+, which reinforces this assertion. The detection of SiF_4 explains the earlier observation,[13] and the result of this work, that the weight remaining after a TGA experiment conducted up to high temperatures is always less than the original silicon oxide weight uptake as measured gravimetrically.

Nafion®–[SiO_2/DEDMS-post-reacted]. For this hybrid, only one sharp mass loss step initiating at ~370°C is observed in *Figure 2*. Although decomposition proceeded more rapidly than for Nafion®–SiO_2, the DEDMS post-reacted sample showed the highest degradation onset temperature. At 450°C a 40% weight loss accumulates; only 6.8% remains at 543°C and 6.0% at 653°C.

Up to ~544°C neither SiF_4 nor SO_2 was detected. There is a peak in SiF_4 evolution between 544°C and 652°C which lies considerably beneath that for Nafion®–SiO_2. Thus, the organic modification of the SiO_2 core by post-reaction with DEDMS retards its degradative reaction with HF. While the SiF_4 curves in the region of the peaks are rather close to each other for Nafion®–H^+ and Nafion®–[SiO_2/DEDMS-*post-reacted*], the onset of this product occurs at a considerably higher temperature for the latter as well as for Nafion®–SiO_2.

The SO_2 profile for Nafion®–[SiO_2/DEDMS-*post-reacted*] (*Figure 4a*) was also considerably depressed beneath those for the other two materials, although the peak at ~580°C is in approximately the same position as that for the others. However, for this hybrid, several methyl group peaks are always present. CH_3 groups are known to detach from Si–C groups at ~500°C.

Thus, it might be generally concluded that, for the Nafion®–[SiO_2/DEDMS-*post-reacted*] hybrid, the silicon oxide core inhibits the thermal degradation of the side-chains while the organic shell inhibits the degradative reaction of the core itself with HF.

Other selected products

Five other bands, in order of increasing absorbance, were detected at 1780, 1380, 1228, 1184 and 1194 cm^{-1}. Absorbance *versus* temperature profiles are in *Figure 5*. Suggested assignments, based on listed references 22–25, are discussed below.

1780 cm^{-1}. This weak band is in the location of C=O stretching such that F atoms are placed near this group. As mentioned, no *substituted* carbonyl fluorides [e.g. $CF_3C(=O)F$, such as those observed at 1957 and 1928 cm^{-1} by Wilkie *et al*. for Nafion®-H^+] are detected in the spectrum for any of our materials. Samms *et al*.[14] detected, via TGA-mass spectrometry, COF_2 whose presence becomes significant at 300°C and is generated in large quantities above 400°C for Nafion®–H^+. Wilkie *et al*. also detected this species. Our degradation products appear to be different substituted carbonyl fluorides; e.g. 1,1,1-trifluoroacetone absorbs at 1780 cm^{-1}. -CF_2-CF_2- groups have a weak peak at ~1790 cm^{-1},[26] which is rather close to the peak in question. The generation of C_xF_y fragments from Nafion®–H^+ was seen to rise sharply between 450°C and 500°C in the TGA-mass spectrometry studies of Samms *et al*.[14]

The absorbance *versus* temperature profiles in *Figure 5a* are somewhat different than those for SO_2 evolution. Absorbance for Nafion®–H^+ rises from insignificance from ~480°C to a maximum at ~597°C. Absorbance of this peak for Nafion®–SiO_2 appears at a lower temperature (~420°C) and rises to a maximum ~552°C. It is noted that the SiF_4 absorbance, which is linked to HF generation, also rises to significance before that for the other two materials. This band, for Nafion®–[SiO_2-DEDMS-*post-reacted*] is detected only after a temperature of ~515°C is reached; a maximum occurs ~580°C. While confusion exists with regard to the assignment of this band, it is clear that, with respect to temperature onset and quantity of evolved product, the Nafion®–[SiO_2/DEDMS-*post-reacted*] hybrid is superior.

1380 cm^{-1} (Figure 5b). Asymmetric stretching in the -SO_2- group of R-SO_2-Cl occurs in the range 1385–1340 cm^{-1} [22]. However, the -SO_2-F group in the Nafion® precursor absorbs at considerably higher wavenumbers, namely 1470 cm^{-1} [25]. It is unknown as to whether a SO_2F radical fragment in the gas phase would absorb at 1380 cm^{-1}. Thionyl fluoride was detected in quantity above 400°C for Nafion®–H^+ via TGA-MS[14], although Wilkie *et al*. do not mention this group in their i.r. analysis. The symmetric bending mode for CH_3 groups occurs at ~1379 cm^{-1} although this group is theoretically not present in Nafion®–H^+ and Nafion®–SiO_2 materials. The origin of this band is unknown.

For Nafion®–H^+, this absorbance appeared after ~385°C and reached a maximum at ~597°C. For Nafion®–SiO_2, the absorbance appeared and increased from ~395°C to a maximum ~552°C. For Nafion®/[SiO_2/DEDMS-*post-reacted*], this product does not appear until ~482°C and occurred in greatest quantity ~580°C. Again, the evolution of the latter hybrid was retarded, with respect to both degradation onset temperature and overall generated quantity, as compared with the other two materials.

1228 cm^{-1} (Figure 5c). The absorbance of this medium intensity peak can be comparable to that for SO_2. This peak falls within the range (1250–1160 cm^{-1}) for asymmetric stretching in SO_2-OH groups[22] and Wilkie *et al*. consider the generation of $\cdot SO_3H$ radicals which later cleave to produce SO_2 in one of their proposed schemes[11]. On the other hand, perfluoro compounds show several C–F stretching peaks over the broad range 1400–1000 cm^{-1}, including an intense peak around 1250 cm^{-1}. It is unlikely that intact R-SO_2-OH species will exist in the gas phase at temperatures greater than 400°C. Therefore, we suggest that it is more probable that this band is due to a C–F-containing fragment.

For Nafion®–H^+, this absorbance appears ~385°C and rises to a maximum ~597°C. For Nafion®–SiO_2, the absorbance appears ~395°C and rises to a maximum at ~552°C. The onset of production of this species for Nafion®–[SiO_2/DEDMS-*post-reacted*] is retarded to ~515°C and the maximum occurs ~580°C

1184 cm^{-1} (Figure 5d) and 1194 cm^{-1}. These bands are discussed together owing to their proximity and because their evolution profiles are almost identical. Since their magnitudes are considerable, the underlying degradation products must be considered as important. These peaks lie within a rather broad range associated with CF_2 stretching vibrations and this is the most probable assignment. Greso *et al*. showed that the IR spectra of a Nafion® sulfonyl fluoride precursor that was modified via reactions with aminopropyltriethoxysilane contains a very strong bimodal absorption envelope with maxima ~1200 and ~1150 cm^{-1} in the region of CF_2 stretching[25].

For both bands, the absorbance for Nafion®–H^+ appears ~365°C and rises to a maximum at ~615°C, and that for Nafion®–SiO_2 appears ~374°C with a maximum at ~593°C. In contrast, the absorbance for Nafion®–[SiO_2/DEDMS-*post-reacted*] only becomes active after ~515°C and reaches a maximum ~580°C. These results reinforce the conclusion that post-reaction of Nafion®–SiO_2 is rather effective in retarding thermal degradation.

I.r. bands unique to Nafion®–[SiO_2/DEDMS-post-reacted]

Here, we discuss six peaks for this hybrid that were absent from the spectra of Nafion®–H^+ and Nafion®–SiO_2. Peak positions, in order of increasing absorbance, are: 817, 3015, 1153, 910, 896 and 977 cm^{-1}. The temperature–product evolution profiles are in *Figures 6* and *7*.

817 cm^{-1} (Figure 6a). This peak lies in the position for Si–C stretching in the Si-$(CH_3)_2$ group. Earlier, we discussed this peak as it appeared in spectra for Nafion®–[SiO_2/DEDMS-*post-reacted*][3] and Nafion®–ORMOSIL hybrids[1]. This feature is very weak for the gas phase product, although this must be due in part to the small fraction of $Si(CH_3)_2$ groups that are bonded in the composite. Recall that the Nafion®–SiO_2 sample weight increase after DEDMS post-reaction was only 4.5%. Other peaks characteristic of the $Si(CH_3)_2$ group, namely at ~850 (CH_3 rocking) and 1263 cm^{-1} (symmetric C–H deformation in CH_3 groups), are not observed which is most likely due to detection insensitivity at this level of product evolution. Greso *et al*. noted twin peaks ~810 cm^{-1} due to S–F stretching vibrations of the SO_2F group in the spectra of the Nafion® SO_2F precursor[25]. In the present study, the only other possible spectral signature of SO_2F radical fragments in the gas phase is the aforementioned band at 1380 cm^{-1}. However, this is considered an unlikely assignment because this frequency is rather low compared with this mode for the intact SO_2F precursor and because the time evolution profiles in *Figure 5*(*b*) and *Figure 6*(*a*) are very dissimilar.

As seen in *Figure 6*(*a*), the gas phase product, considered to be Si-$(CH_3)_2$-containing fragments, becomes significant at ~380°C and rises to maximum evolution at ~580°C. The shoulder at ~480°C indicates a two-step process. With regard to the latter feature, the Si-C bond of Si-CH_3 is known to be stable to ~450°C.

3015 cm^{-1} (Figure 6b). The absorbance *versus* temperature plot for this minor product begins to rise slowly at ~250°C with a maximum at ~480°C followed by a slow decrease. This peak is most likely due to stretching within CH_3 groups although the situation is somewhat unclear, as will be discussed. If the methyl portion of the Si–CH_3 group is detached at a high temperature, a number of possible products could form. Bands of alkane fragments (CH_3, CH_2, CH) occur in the region 3000–2800 cm^{-1} for C–H stretching (see Ref. 15, p. 102) and the 3015 cm^{-1} band seen in *Figure 3c* is not far removed from this region. For polar substituents (X) the frequency is higher for CH_nX (n = 1–3) groups when X is a strong-electron attractor such as F-containing species. We again recall that the Si–C bond of Si-CH_3 is known to be stable to ~450°C, whereas the 3015 cm^{-1} peak appears at the considerably lower temperature of ~250°C.

We suggest that this peak is due to methyl groups because only special C–H stretches absorb in the region 3100–3000 cm^{-1}. Perhaps a small fraction of Si–C group cleavage is possible at lower temperatures due to bond perturbations in the chemically-complicated Nafion® nanoenvironment. It is not possible to form =CH groups (as in alkenes absorbing at ~3100–3000 cm^{-1}) in a SiC(H)(=CXY) group, where X and Y are organic moieties coming from fluorocarbons and hydrocarbons issuing from other methyl groups, without cleavage of Si–C bonds at other locations. Finally, CH_4 vapour shows strong absorbances in the region 3100–2900 cm^{-1} and 1350-1250 cm^{-1}, which fact further complicates this analysis.

While this absorbance is weak, it is detected over a broad temperature range as compared with other bands that are unique to this hybrid, save for the 817 cm^{-1} band which also implicates methyl groups.

1153 cm^{-1} (Figure 6c) The onset temperature and position of the maximum for this band are the same as those for the 1380 cm^{-1} peak. The broad range for –SO_2– asymmetric stretching around 1250–1160 cm^{-1} in R–SO_2–OH species (see Ref. 15, p. 198) is in the vicinity of this peak. It was mentioned earlier that the 1228 cm^{-1} medium intensity peak also falls within this range, although, as in the earlier discussion of this peak, we consider that R–SO_2–OH species are unlikely. An alternate consideration is based on the fact that sulfones, R–SO_2–R′ have symmetric stretching vibrations in the region 1160–1135 cm^{-1} (see Ref. 15, p. 198). Given the presence of CH_3 groups, it might be reasonable to consider R and R′ to be CH_3 and/or fluorocarbon groups. This peak is seen to abruptly appear at ~480°C, have a maximum at ~580°C, and decrease more slowly afterwards.

910 cm^{-1} (Figure 6d). –CH=CH_2 vinyl compounds have a very strong band for a CH_2 out-of-plane bending deformation in the region ~995–905 cm^{-1} (see Ref. 15, p. 106). In addition, =CH stretching is around

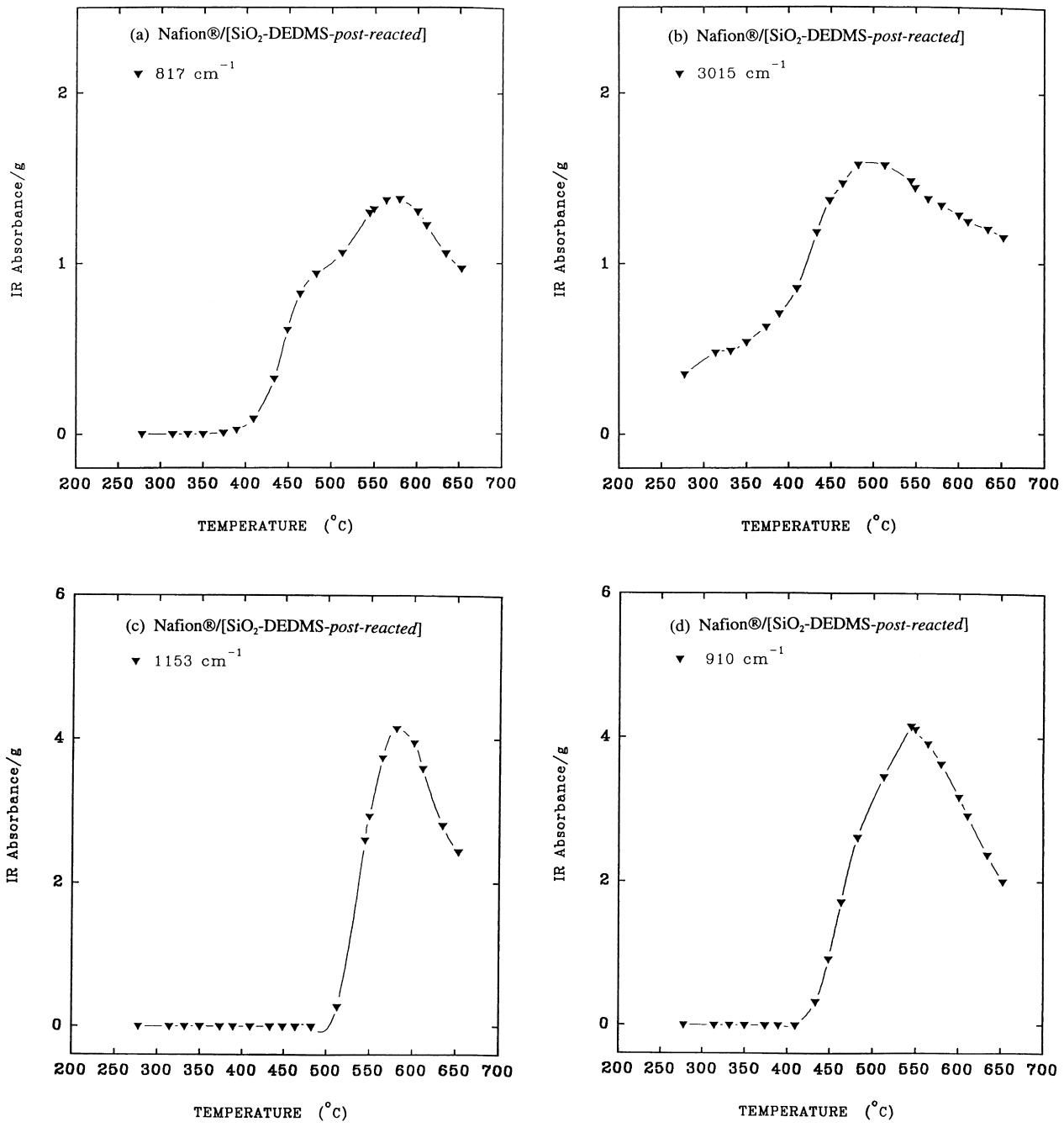

Figure 6 I.r. absorbance of bands unique to Nafion®–[SiO_2/DEDMS-*post-reacted*] *versus* temperature

3030–2980 cm^{-1}, which is consistent with the peak at 3015 cm^{-1}. The formation of such products could be related to the presence of the methyl groups in the composite. This peak appears ~410°C, has a maximum at ~544°C, and the degradation profile is rather broad.

896 cm^{-1} (Figure 7a). This might be the signature of a different substituted $-CH{=}CH_2$ product. Commensurate with this idea is that fact that in *Figure 7a*, as in *Figure 6d*, the absorbance starts at ~410°C and has a maximum at ~544°C.

977 cm^{-1} (Figure 7b). This is the most intense band (see *Figure 3c*) of the six that are unique to the Nafion®–[SiO_2/DEDMS-*post-reacted*] hybrid. Undegraded Nafion® has two strong peaks at ~980 and 965 cm^{-1} due to the stretching vibrations of the two –C–O–C– groups in the side-chains[26]. In recent studies, we have assigned the 965 cm^{-1} component to the perfluoroether group closest to the sulfonate group[27]. Samms *et al.*[14] report an onset temperature for the generation of $C_xF_yO_z$, compounds at around 450°C. Moreover, the mass spectrum-based temperature profile is very similar to the i.r.-based profile seen in *Figure 7b*. Therefore, it would be natural to account for the ether links in the side-chains by this peak. On the other hand, this band is absent for the Nafion®–H^+ and Nafion®–SiO_2 samples. According to Wilkie *et al.*, no -C–O–C- groups appear among the degradation products after the initial step of C–S bond cleavage and carbonyl fluorides begin to appear. Furthermore, it is noted, with reference to *Figures 4a* and *7b*, that the fragment whose signature is the 977 cm^{-1} band, appears at a temperature

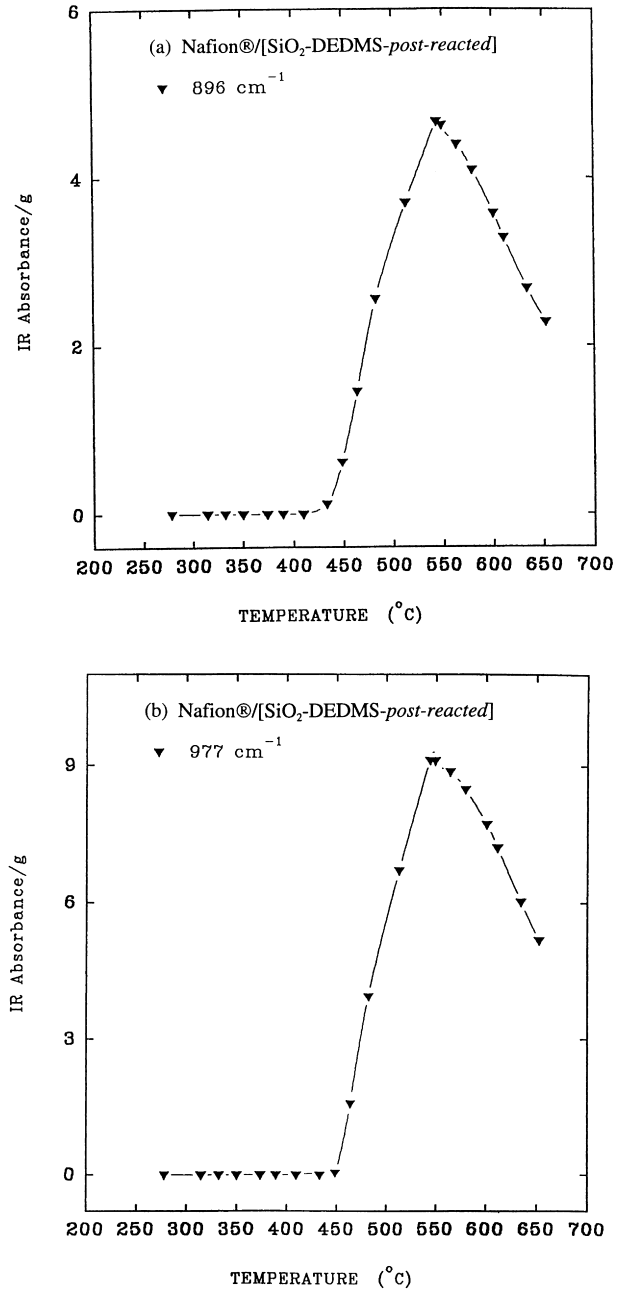

Figure 7 Same as in *Figure 6*.

that is 100°C lower than that at which SO_2 evolution commences for this particular hybrid, whereas it is thought that the sulfonate endgroup should be the first to detach. The previously-discussed $-CH=CH_2$ vinyl group vibration and C–H out-of-plane deformation vibration in $-CH=CH-$ groups at ~980–965 cm^{-1} are also in this vicinity. It is significant with regard to these latter considerations that *Figure 7b* is very similar in pattern to, and has the same maximum as the graphs in *Figures 6d* and *7a*. The absorbance rises abruptly at ~448°C and has a maximum ~544°C. Finally, a peak for Si–F stretching in this vicinity cannot be ruled out. Si–F bonds could be formed pursuant to the liberation of CH_3 groups.

CONCLUSIONS

Integrated TGA–*FT*i.r. analysis revealed the fingerprints of a number of molecular fragments that evolved during the thermal degradation of Nafion®–SiO_2 and Nafion®–(SiO_2–organically modified) hybrids that were produced via *in situ* sol–gel processes. It was demonstrated that the degradation pathway for this polymer is altered by incorporation of these Si-containing nanophases. While the gravimetric loss is multistep for unfilled Nafion®–H^+ and Nafion®–SiO_2, it appears as a single-step process for the Nafion®–[SiO_2/DEDMS-*post-reacted*] hybrid, which has the greatest thermal stability.

The considerable inhibition of SO_2 evolution for both hybrids is rationalized in terms of side-chains that are immobilized within silicon oxide cages that block reactions involving $-SO_3$ groups. However, these cages are ultimately degraded by their reaction with HF that is generated in the degradation process. Insertion of silicon oxide molecular fragments between side-chains might disrupt the physical cross-linking due to side-chain aggregation so that cage degradation by HF causes decomposition that is more abrupt than that for unfilled Nafion®–H^+. On the other hand, organic modification of the SiO_2 core by post-reaction with DEDMS retards its degradation by HF. Detected SiF_4 derives from reactions between evolved HF and Nafion®-incorporated SiO_2 as well as with Si in the TGA quartz tube. Altogether, the amount of SiF_4 evolved is directly related to the amount of HF issuing from the degrading polymer. Evidence for particular substituted carbonyl fluorides is present. It is unlikely that intact $R-SO_2-OH$ groups, or perfluoroalkylether groups issuing from the side-chains of Nafion®, exist as gas phase products. CF_2-containing fragments are detected and the evolution of these products is greatly retarded for the Nafion®–[SiO_2/DEDMS-*post-reacted*] hybrid. Si-CH_3 groups in small quantity, CH_3 groups and/or $-CH=CH_2$ vinyl compounds formed from liberated CH_3 groups, appear among the degradation products for the latter hybrid. While the origins of some peaks are in question owing to spectral complexity, it is nonetheless clear that the Nafion®–[SiO_2/DEDMS-*post-reacted*] hybrid is superior with respect to high degradation onset temperature and low quantity of a number of evolved products.

ACKNOWLEDGEMENTS

This material is based partly upon work supported by a grant from the National Science Foundation/Electric Power Research Institute (Advanced Polymeric Materials: DMR-9211963). This work was also sponsored in part by the Air Force Office of Scientific Research, Air Force Systems Command, USAF, under grant number AFOSR F49620-93-1-0189, and also the Mississippi NSF-EPSCoR program. The donation of Nafion® membranes by the E.I. DuPont Co., through the efforts of J.T. Keating, is appreciated.

REFERENCES

1. Deng, Q., Moore, R. B. and Mauritz, K. A., *Chem. Mater.*, 1995, **7**, 2259.
2. Gierke, T. D., Munn, G. E. and Wilson, F. C., *J. Polym. Sci. B., Polym. Phys. Ed.*, 1981, **19**, 1687.
3. Deng, Q., Mauritz, K. A. and Moore, R. B., in *Hybrid Organic–Inorganic Composites, ACS Symp. Ser. 585*, eds J. E. Mark, P. A. Bianconi and C. Y.-C. Lee, ACS, Washington, DC, 1995, Chap. 7.
4. Mauritz, K. A., Stefanithis, I. D., Davis, S. V., Scheetz, R. W., Pope, R. K., Wilkes, G. L. and Huang, H.-H., *J. Appl. Polym. Sci.*, 1995, **55**, 181.

5. Deng, Q., Cable, K. M., Moore, R. B. and Mauritz, K. A., *J. Polym. Sci. B., Polym. Phys. Ed.*, 1996, **34**, 1917.
6. Deng, Q., Jarrett, W., Moore, R. B. and Mauritz, K. A., *J. Sol–gel Sci and Technol*., 1996, **7**, 177.
7. Deng, Q., Hu, Y., Moore, R. B., McCormick, C. L. and Mauritz, K. A., *Chem. Mater*., 1997, **9**, 36.
8. Deng, Q., Moore, R. B. and Mauritz, K. A., *J. Appl. Polym. Sci*., 1998, **68**, 747.
9. Provder, T., Urban, M. W., Barth, H. G., eds. *Hyphenated Techniques in Polymer Characterization: Thermal–spectroscopic and Other Methods, ACS Symp. Ser. 581*. ACS, Washington, DC, 1994.
10. Johnson, D. J. and Compton, D. A. C., *Amer. Lab.* 1990, Jan., 37.
11. Wilkie, C. A., Thomsen, J. R. and Mittleman, M. L., *J. Appl. Polym. Sci.*, 1991, **42**, 901.
12. Feldheim, D. L., Lawson, D. R. and Martin, C. R., *J. Polym. Sci.*, 1993, **B31**, 953.
13. Stefanithis, I. D. and Mauritz, K. A., *Macromolecules*, 1990, **23**, 2397.
14. Samms, S. R., Wasmus, S. and Savinell, R. F., *J. Electrochem. Soc.*, 1996, **143**, 1498.
15. Chandrasiri, J. A., Roberts, D. E. and Wilkie, C. A., *Polym. Degrad. Stab.*, 1994, **45**, 97.
16. Wilkie, C. A. and Mittleman, M. L., in *Hyphenated Techniques in Polymer Characterization*, eds, Provder, T., Urban, M. W. and Barth, H. G. ACS Symp. Ser. No. 581, ACS, Washington, DC, 116, 1994.
17. Suzuki, M. and Wilkie, C. A., *Polym. Degrad. Stab.*, 1995, **47**, 223.
18. Suzuki, M. and Wilkie, C. A., *Polym. Degrad. Stab.*, 1995, **47**, 217.
19. Wilkie, C. A., Suzuki, M., Dong, X., Deacon, C., Chandrasiri, J. A. and Xue, T. J., *Polym. Degrad. Stab.*, 1996, **54**, 117.
20. Xue, T. J. and Wilkie, C. A., *Polym. Degrad. Stab.*, 1997, **56**, 109.
21. Xue, T. J., Mckinney, M. A. and Wilkie, C. A., *Polym. Degrad. Stab.*, 1997, **58**, 193.
22. Conley, R. T., *Infrared Spectroscopy*; 2nd edn. Allyn and Bacon, Boston, 1972.
23. Bellamy, L. J., *The Infra-red Spectra of Complex Molecules*. Chapman and Hall, London, 1975.
24. Silverstein, R. M., Bassler, G. C. and Morrill, T. C., *Spectrometric Identification of Organic Compounds*, 5th edn. Wiley, New York, 1991.
25. Greso, A. J., Moore, R. B., Cable, K. M., Jarrett, W. L. and Mauritz, K. A., *Polymer*, 1997, **88**(6), 1345.
26. Falk, M., in *Perfluorinated Ionomer Membranes, ACS Symp. Ser. 180*, eds, Eisenberg, A. and Yeager, H. L. ACS, Washington, DC, 1982, Chap. 8.
27. Cable, K. M., Mauritz, K. A. and Moore, R. B., *J. Polym. Sci. B: Polym. Phys.*, 1995, **33**, 1065.